Single-crystal elasticity of wadsleyites, β-Mg$_2$SiO$_4$, containing 0.37–1.66 wt.% H$_2$O

Z. Mao [a,*], S.D. Jacobsen [b], F. Jiang [a], J.R. Smyth [c], C.M. Holl [b], D.J. Frost [d], T.S. Duffy [a]

[a] *Princeton University, Department of Geosciences, Princeton, NJ 08540, USA*
[b] *Northwestern University, Department of Earth and Planetary Sciences, Evanston, IL 60208, USA*
[c] *University of Colorado, Department of Geological Sciences, Boulder, CO 80309, USA*
[d] *Bayerisches Geoinstitut, Universität Bayreuth, Bayreuth 95440, Germany*

Abstract

The presence of hydrogen can affect elastic properties and seismic velocities of minerals in the Earth's upper mantle. In this study, the second-order elastic constants of hydrous wadsleyites containing 0.37, 0.84, and 1.66 wt.% H$_2$O were determined by Brillouin scattering at ambient conditions. Measurements were performed on at least three independent crystal planes for each composition. The aggregate bulk modulus, K_{S0}, and shear modulus, G_0, were calculated using VRH (Voigt–Reuss–Hill) averages. The results are: $K_{S0} = 165.4(9)$ GPa, $G_0 = 108.6(6)$ GPa for wadsleyite with 0.37 wt.% H$_2$O; $K_{S0} = 160.3(7)$ GPa, $G_0 = 105.3(6)$ GPa for 0.84 wt.% H$_2$O; $K_{S0} = 149.2(6)$ GPa, $G_0 = 98.6(4)$ GPa for 1.66 wt.% H$_2$O. We find that the bulk and shear moduli of hydrous wadsleyites decrease linearly with water content according to the following relations (in GPa): $K_{S0} = 170.9(9) - 13.0(8)C_{H2O}$, $G_0 = 111.7(6) - 7.8(4)C_{H2O}$, where C_{H2O} is the H$_2$O weight percentage. Compared with anhydrous wadsleyite, addition of 1 wt.% H$_2$O will lead to a 7.6% decrease in the bulk modulus, and a 7.0% decrease in the shear modulus. Using these results, we examine the velocity contrast between hydrous olivine and wadsleyite at ambient conditions for an Fe-free system assuming an H$_2$O partition coefficient between wadsleyite and olivine of 3. The velocity contrast in compressional and shear velocity between wadsleyite and olivine ranges from 12 to 13% for an H$_2$O-free system to 7–8% for wadsleyite containing 1.5 wt.% H$_2$O. Thus, the magnitude of the seismic velocity change at 410-km depth can be expected to be sensitive to the presence of H$_2$O in olivine polymorphs.
© 2007 Elsevier B.V. All rights reserved.

Keywords: Hydrous wadsleyite; Elasticity; Brillouin scattering; Velocity contrast; Transition zone

1. Introduction

Wadsleyite (β-Mg$_2$SiO$_4$) is the high-pressure polymorph of olivine that is expected to be a dominant mineral in the Earth's mantle from 410 km to 520 km depth. Previous studies show that wadsleyite can incorporate variable amounts of water as structurally bound hydroxyl (OH), up to a maximum of 3.3 wt.% H$_2$O if every non-silicate oxygen site in the structure is protonated (Smyth, 1987, 1994). Wadsleyite has the greatest hydrogen storage capacity among the olivine polymorphs. At transition

* Corresponding author.
 E-mail address: zhumao@princeton.edu (Z. Mao).

zone conditions (~ 15 GPa, 1400 °C), the water content of wadsleyite coexisting with hydrous melt is about 0.9 wt.% (Demouchy et al., 2005). Ringwoodite, which is the stable olivine polymorph from 520 km to 660 km depth, can also incorporate 2–3 wt.% H_2O below 1100 °C and up to ~ 0.3 wt.% H_2O at 1500–1600 °C (Kohlstedt et al., 1996; Ohtani et al., 2000). Thus, the Earth's transition zone, which is dominated by ringwoodite and wadsleyite, could contain a large water reservoir perhaps even exceeding the mass of the hydrosphere (Smyth, 1994).

Small amounts of H_2O can strongly influence a number of important physical properties of mantle minerals. Hydration is expected to alter the thickness and depth of the olivine to wadsleyite phase transition (e.g., (Wood, 1995; Chen et al., 2002; Smyth and Frost, 2002)), promote partial melting (Hirschmann, 2006), and alter rheological and transport properties (Chen et al., 1998; Huang et al., 2005; Karato, 2006). Incorporation of H_2O will also affect elastic properties (Jacobsen, 2006). Knowledge of the elastic properties of wadsleyite is crucial for interpreting seismic profiles and tomographic images of the mantle and identifying potential water-rich regions. To date, the elasticity of hydrous wadsleyite has been investigated only by static compression studies (Yusa and Inoue, 1997; Smyth et al., 2005; Holl et al., in press). Yusa and Inoue (1997) reports that incorporation of 2.5 wt.% of H_2O leads to a 15% reduction in the isothermal bulk modulus, K_{T0}, for a fixed value of the pressure derivative, $(\partial K_T / \partial P)_{T0} = K'_{T0}$. However, static compression studies on various hydrous olivine polymorphs (Smyth et al., 2004, 2005; Holl et al., in press; Manghnani et al., 2005) show that incorporation of water may increase K'_{T0}. Furthermore, the shear modulus cannot be determined from static compression.

In this study, we use Brillouin scattering to determine the full elastic tensor of hydrous wadsleyite and place bounds on the bulk and shear moduli of polycrystalline aggregates. The variation of elastic moduli of wadsleyite as a function of H_2O content was obtained by measuring three different compositions containing 0.37(4) wt.%, 0.84(8) wt.% and 1.66(17) wt.% H_2O, respectively. The potential effect of hydration on the velocity contrast between olivine and wadsleyite is examined. Variations in aggregate elastic properties of olivine polymorphs are systematically evaluated as a function of phase, Fe content, and hydration.

2. Experimental details

2.1. Synthesis and characterization

Single crystals of hydrous wadsleyite, β-Mg_2SiO_4, were synthesized in the 1200-ton Hymag or Sumitomo

multianvil presses at the Bayerisches Geoinstitut, Bayreuth, Germany. Starting materials consisted of mixed oxide powders; MgO plus SiO_2 with slight excess silica and water added as brucite, $Mg(OH)_2$. Runs were carried out in welded platinum capsules at conditions of 14–16 GPa and 1200–1400 °C with heating durations of at least one h and rapid quenching. Samples were selected for Brillouin scattering from runs WH833 (Jacobsen et al., 2005), SS0401(Holl et al., in press), and a new synthesis run, WH2120.

Lattice parameters for representative crystals from each run (Table 1) were determined by single-crystal X-ray diffraction using eight-position centering of 15–20 low-angle reflections on either the Huber four-circle diffractometer in Bayreuth (samples WH833 and WH2120) or the Bruker P4 four-circle diffractometer in the Mineral Structures Laboratory at the University of Colorado (sample SS0401). For selected samples from WH833 to WH2120, additional energy dispersive single-crystal diffraction measurements were carried out at the X17C beamline of the National Synchrotron Light Source (Hu et al., 1993) to determine the orientations of polished platelets. For SS0401, selected orientations were determined at the University of Colorado.

Previous studies (Smyth et al., 1997; Kudoh and Inoue, 1999) have reported a monoclinic distortion in hydrous wadsleyite. The cause of monoclinic symmetry in hydrous wadsleyite remains unresolved, but it has been speculated to result from cation vacancy ordering (Smyth et al., 1997), stacking disorder of distinct structural modules (Kudoh and Inoue, 1999), or polysynthetic twinning (Holl et al., in press). Among six hydrous wadsleyite runs studied by Jacobsen et al. (2005), only samples with water contents greater than about 0.5 wt.% H_2O displayed the monoclinic symmetry. In this study, samples from run WH833 are orthorhombic with average $\beta = 90.002(3)°$ (Jacobsen et al., 2005). Samples from run WH2120 display a slight monoclinic distortion with average $\beta = 90.044(5)°$. Samples

Table 1
H_2O content and crystallographic data of hydrous wadsleyite samples

	WH833 [a]	WH2120	SS0401 [b]
H_2O (wt.%)	0.37(4)	0.84(8)	1.66(17)
a (Å)	5.6941(2)	5.6888(6)	5.6807(3)
b (Å)	11.4597(3)	11.4830(8)	11.5243(6)
c (Å)	8.2556(2)	8.2523(6)	8.2515(6)
V (Å^3)	538.70(3)	539.08(8)	540.20(5)
ρ (g/cm^3)	3.453(2)	3.435(7)	3.395(10)

Numbers in parentheses are one-standard deviation uncertainties in the last digit(s).
[a] Lattice parameters of WH833 are from Jacobsen et al. (2005).
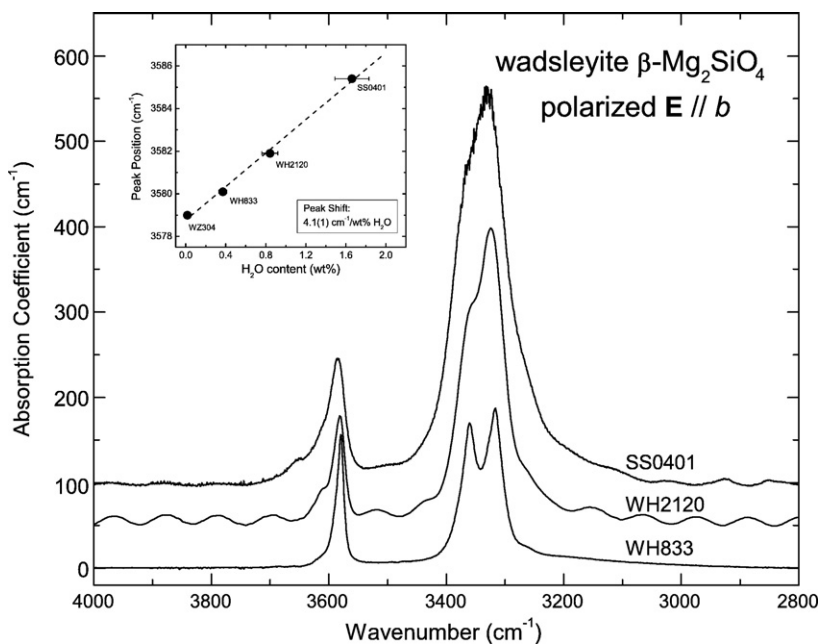[b] Lattice parameters of SS0401 are from Holl et al. (in press).

Fig. 1. Polarized IR spectra with E//b for the wadsleyite samples studied by Brillouin spectroscopy: WH833 (after Jacobsen et al. (2005)), WH2120, and SS0401. Spectra are normalized and baseline corrected but otherwise untreated. For clarity, spectra WH2120 and SS0401 are shifted by 50 and 100 cm^{-1}, respectively. The main bands at 3300–3400 cm^{-1} are not resolved for high-water content samples WH2120 and SS0401 (sample thickness was ∼30 μm), so H$_2$O contents for these samples were estimated from b/a axial ratios using the relative calibration of Jacobsen et al. (2005). The absorption peak at 3580 cm^{-1} shifts to higher wavenumber with increasing water content (inset). The fit also includes a low H$_2$O-content sample WZ304 (∼150 ppm wt. H$_2$O) from Jacobsen et al. (2005).

from run SS0401 display β angles of up to 90.09(2)°. For the present Brillouin scattering measurements, these slight distortions are not considered and orthorhombic (*Imma*) symmetry is assumed.

2.2. Water contents

The concentration of hydroxyl (OH) in hydrous wadsleyite is commonly reported in wt.% H$_2$O or parts per million by weight (ppm wt), where 1 wt.% H$_2$O = 10,000 ppm wt H$_2$O. Estimating the water contents is problematic because an absolute calibration for OH specific to wadsleyite has not been established for either spectroscopic (IR) or secondary ion mass spectrometry (SIMS). Polarized Fourier transform infrared (FTIR) spectroscopy was used to estimate the water content of sample WH833 using the calibration of Libowitzky and Rossman (1997), resulting in 0.37 wt.% as the sum from polarized measurements with E//a, E//b, and E//c (Jacobsen et al., 2005). Spectra for sample WH833 with E//b are shown in Fig. 1. Polarized IR spectra for samples WH2120 and SS0401 are also shown in Fig. 1, and illustrate the typical problem of using IR to study wadsleyite. Namely, the dominant absorption band pair at 3300–3400 cm^{-1}

cannot be resolved because of the high-water content (>0.5 wt.%) in these samples. The spectra in Fig. 1 were obtained from 30-micron thick plates, but the use of thinner plates measuring ∼10 μm thickness for SS0401 also resulted in complete absorption at 3300–3400 cm^{-1}. Therefore, the relationship between the b/a axial ratio and estimated water content from Jacobsen et al. (2005) was used to calculate the water content of WH2120 and SS0401. This relationship, $b/a = 2.008 + 1.25 \times 10^{-6} C_{H2O}$ (in ppm wt) uses water contents from IR at lower concentrations and SIMS data at higher concentrations. The correlation uses b/a because the b axis of wadsleyite increases systematically with water content and the a axis decreases systematically with increasing water content. Although there is also a clear positive volume of hydration (i.e. volume increases with water content), by using b/a individual measurements are not subject to absolute uncertainty in the volume, which may vary from one diffractometer to another. The b/a relationship results in 0.84 wt.% H$_2$O for sample WH2120 and 1.66 wt.% H$_2$O for SS0401. Water contents for all samples studied by Brillouin spectroscopy in this study are listed in Table 1. Because there is no absolute calibration for water in wasleyite, we have chosen to use arbitrary 10%
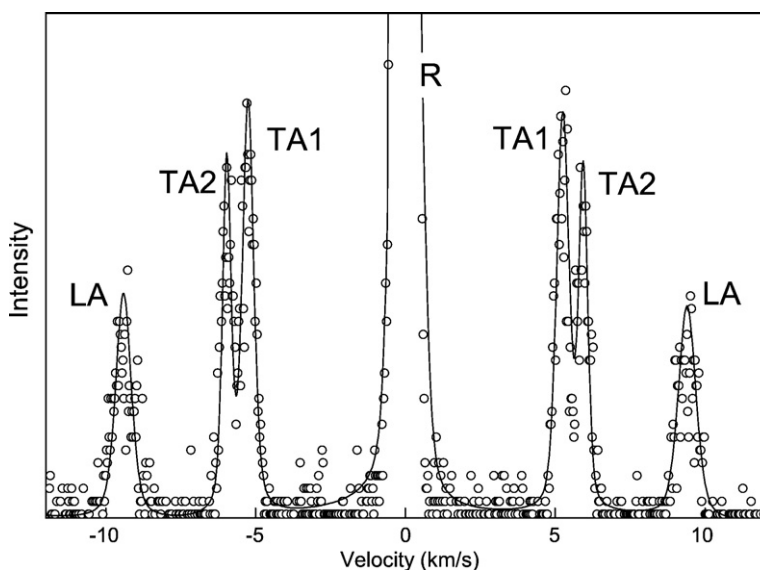
Fig. 2. Example Brillouin spectrum of wadsleyite with 0.84 wt.% H_2O (sample WH2120). LA: longitudinal mode; TA1: slow shear mode; TA2: fast shear mode; R: elastic mode; open circles: measured data; solid line: fitting results.

error bars in subsequent figures and in calculation of density.

2.3. Variation of density with water content

Measured unit cell volumes and water contents were used to calculate the variation of density (Fig. S1 in the Appendix). A nominally anhydrous sample (WS3056) containing about 50 ppm wt H_2O with $\rho_{calc}=3.472(1)$ g/cm^3 from the study of Jacobsen et al. (2005) is used for comparison. This sample represents the least amount of water from attempts to synthesize wadsleyite without hydroxyl (Jacobsen et al., 2005). Formula weights were calculated according to the stoichiometry Mg_{2-x} $H_{2x}SiO_4$, where $2x$ was determined as discussed in Section 2.2 and full Si occupancy is assumed. The decrease in density of wadsleyite at STP varies as:

$$\rho = 3.472(1) - 0.046(2) \times C_{H_2O} \qquad (1)$$

where density is given in g/cm^3 and C_{H_2O} is the H_2O weight percentage.

2.4. Raman spectroscopy

Raman spectra were measured for all samples at ambient conditions. Up to 22 Raman modes were observed for a given sample (Fig. S2 in the Appendix). The peak positions obtained for the sample with 1.66 wt.% H_2O are generally in good agreement with a previous study (Kleppe et al., 2001) which had a nearly identical

water content. In the range 200–1100 cm^{-1}, most of modes show a subtle decrease in frequency with water content. Lattice mode frequencies typically decrease by ~ 3 cm^{-1} from nominally anhydrous wadsleyite to samples with 1.66 wt.% H_2O. We also observed three OH modes for each composition (Table S1 in the Appendix). Compared with (Kleppe et al., 2001), our OH modes occur at slightly lower frequencies. For the OH doublet at 3321 cm^{-1} and 3582 cm^{-1}, the frequency increases by 7.4 cm^{-1} and 8.8 cm^{-1} respectively from 0.37 to 1.66 wt.% H_2O. The frequency increases by 2.6 cm^{-1} for the 3582 cm^{-1} mode over the range of water content. Thus, water has a weak but detectable effect on Raman frequencies, with lattice modes generally decreasing and OH modes increasing as a function of H_2O content.

2.5. Brillouin spectroscopy

All samples were double-side polished to thicknesses ranging from 30 μm to 200 μm. A large-opening diamond anvil cell was used to hold platelets that were less than 50 μm thick. Since all the experiments were performed at ambient conditions, no pressure was applied to the diamond cell. A special cell was designed to hold platelets thicker than 50 μm. This holder was made from a stainless steel gasket with a 1-mm hole in the center. The crystal platelet was loaded into the center of the gasket hole and sandwiched between two glass slides.

Brillouin spectra were measured in a forward scattering geometry at ambient conditions using a six-pass
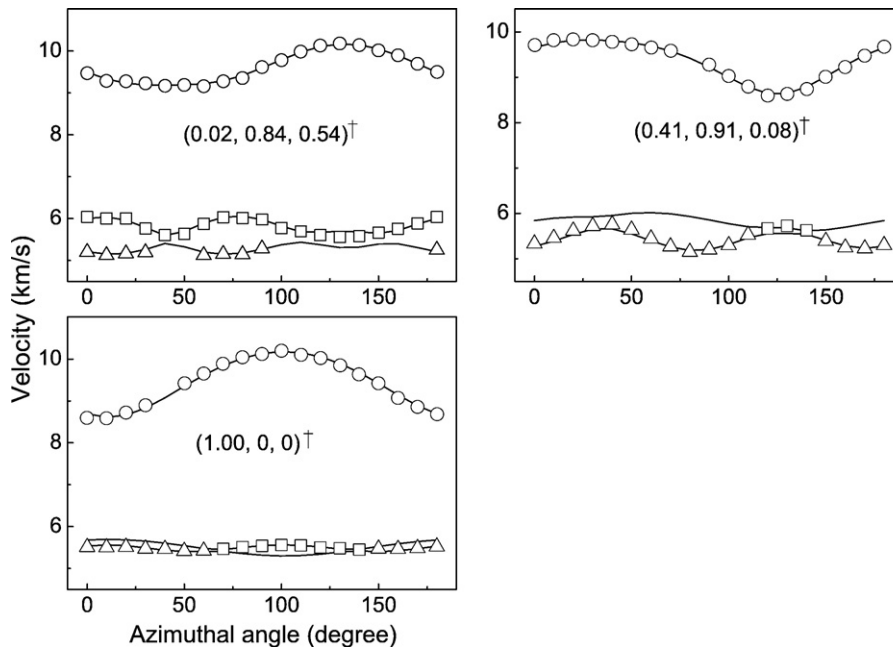
Fig. 3. Measured compressional and shear wave velocities of hydrous wadsleyite as a function of direction for WH833 with 0.37 wt.% H_2O. Symbols represent experimental data. Circles: compressional velocities; squares: fast shear velocity; triangles: slow shear velocity. Solid lines are best-fitting results. The crystallographic orientation of each platelet is indicated on the graph. † indicates platelets for which X-ray diffraction was performed.

Sandercock tandem Fabry–Perot interferometer. The sample was probed using a solid state laser with a wavelength 532.15nm and power of about 150mW. For a symmetric scattering geometry, acoustic velocities are related to the measured Brillouin frequency shift Δv_B by:

$$v = \frac{\Delta v_B \lambda_0}{2\sin(\theta/2)} \qquad (2)$$

where v is the acoustic velocity, λ_0 is the incident wavelength, θ is the external scattering angle (70° in this study). Further details of the Brillouin system are provided elsewhere (Speziale and Duffy, 2002).

For each platelet, we collected spectra at 10° steps in a total of 19 directions over a range of 180°. The average collection time ranged from 30 to 50 min/spectrum. Fig. 2 shows an example Brillouin spectrum of hydrous wadsleyite. One quasi-longitudinal and two quasi-transverse modes were observed in most directions. The three acoustic modes are usually clearly separated. All spectra had a high signal-to-noise ratio. The uncertainty of the measurement was within 0.5 to 1% of the measured velocities.

3. Results

Although some of our samples display a slightly monoclinic distortion which would require character-

ization of 13 elastic constants, the Brillouin data were fitted assuming orthorhombic symmetry because the angular deviation from 90° is small (see Section 2.1). In this case, nine independent elastic constants are needed to characterize each sample. The orientation of each platelet can be described by three Eulerian angles (θ, ϕ, χ) that relate the laboratory coordinate system to the crystal coordinate system (Shimisu, 1995). The Eulerian angles together with an azimuthal angle determine the phonon propagation direction which can be expressed by the direction cosines, n_i. In total, there are $9+3k$ unknown parameters (9 elastic constants, k platelets, $3k$ Eulerian angles). These were obtained by fitting the velocity data for all platelets of a given composition simultaneously using Christoffel's equation (Every, 1980):

$$\det|C_{ijkl}n_j n_l - \rho v^2 \delta_{ik}| = 0 \qquad (3)$$

where, ρ is the density, v is the phonon velocity, n_i are the direction cosines of the phonon propagation direction, and the C_{ijkl} are the elastic constants in full suffix notation. The velocity data were inverted using the non-linear least-squares Levenberg–Marquardt method (Press et al., 1988). Orientations of some platelets (6 out of 10 total) were determined by single-crystal X-ray diffraction at the X17C beamline of the
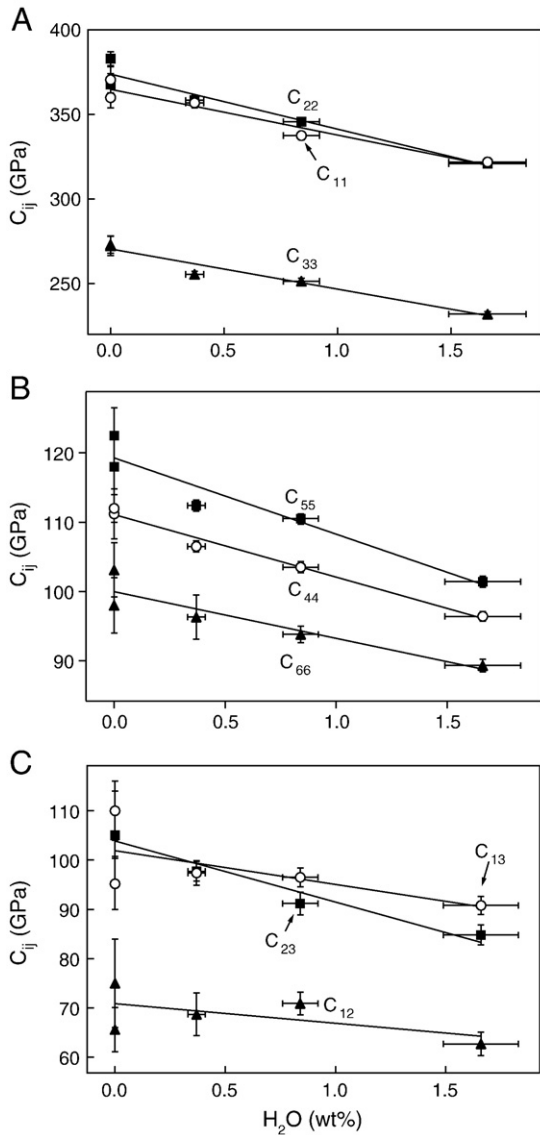
Fig. 4. Single-crystal elastic moduli of Mg_2SiO_4 hydrous wadsleyite as a function of water content. Data for (nominally) anhydrous wadsleyite are from Sawamoto et al. (1984) and Zha et al. (1997). Error bars are smaller than symbols when not shown.

National Synchrotron Light Source (Hu et al., 1993) and/or the Mineral Structures Laboratory at the University of Colorado at Boulder. The starting values used for the non-linear least-squares inversion were the elastic constants of anhydrous wadsleyite (Sawamoto et al., 1984; Zha et al., 1997) and the subset of crystal orientations measured by X-ray diffraction.

Table S2 in the Appendix shows the best-fitting C_{ij} values where the compact Voigt notation (Nye, 1985) for the elastic tensor is adopted. The uncertainty of the recovered Eulerain angles is typically within ±2°. The

difference between the recovered and initial X-ray crystal orientations is also 2° on average but can be as large as 5°. Some uncertainty is likely introduced due to the remounting of the assembly holding the crystal platelets between the X-ray and Brillouin measurement. In addition, covariance among the Eulerain angles for a given plane may also contribute to uncertainty in recovered orientations. Fig. 3 shows the experimentally obtained velocity data together with values calculated from the best-fitting elastic constants for WH833 with 0.37 wt.% H_2O. For WH2021 and SS0401, results are presented in Fig. S3. The root-mean-square (RMS) deviation (Table S2 in the Appendix) between measured and calculated acoustic velocities ranges from 39 m/s to 51 m/s. This indicates excellent agreement between the measured and calculated acoustic velocities.

In Fig. 4, variation of individual elastic moduli with water content is shown. Linear fits to the C_{ij} values including nominally anhydrous compositions (Sawamoto et al., 1984; Zha et al., 1997) as a function of H_2O content are shown by the solid lines. Longitudinal moduli C_{11}, C_{22}, C_{33}, shear modulus, C_{44}, and off-diagonal modulus, C_{23}, display a well-defined linear decrease with H_2O content. Due largely to the difference between anhydrous elastic constants of Sawamoto et al. (1984) and Zha et al. (1997), the trends for C_{55}, C_{66}, C_{12}, and C_{13} are less certain. C_{23} is the elastic modulus most strongly affected by incorporation of water. It decreases 20% from 0% to 1.66 wt.% H_2O. On the other hand, C_{12} only shows a weak dependence on water content. The longitudinal (C_{11}, C_{22}, C_{33}) and shear (C_{44}, C_{55}, C_{66}) moduli all show similar decreases with water content.

The covariance matrix was calculated to evaluate the trade-off among recovered pairs of elastic constants (Press et al., 1988; Brown et al., 1996). In general, trade-off coefficients for longitudinal and shear moduli are small and indicate the elastic moduli are well-resolved. C_{12} is the most poorly constrained elastic modulus. For sample WH833 (0.37 wt.% H_2O), C_{12} shows strongest dependence on the value of C_{11}, C_{22}, C_{33}, and C_{66}. For sample WH2120 (0.84 wt.% H_2O), C_{12} depends on the value of C_{13}, C_{22}, C_{33} and C_{66}. The trade-off between C_{11} and C_{66}, C_{33} and C_{66} for sample WH833, C_{11} and C_{12}, C_{23} and C_{66}, C_{23} and C_{13} for sample WH2120 are also greater than average. The crystal orientations sampled for WH833 (0.37 wt.% H_2O) are relatively deficient in directions normal to the c axis, and this may be responsible for some of the scatter in individual C_{ij}s (Fig. 4). Nevertheless, aggregate moduli obtained from the single-crystal elastic constants are likely well determined because trade-off errors tend to cancel during averaging (Zha et al., 1996).

4. Discussion

4.1. Aggregate elastic moduli of hydrous wadsleyite

Table 2 shows the VRH (Voigt–Reuss–Hill) averages for the adiabatic elastic moduli of randomly oriented polycrystalline aggregates of hydrous wadsleyite. Also shown are VRH average compressional and shear wave velocities. The bulk modulus and shear modulus decrease linearly with water content (Fig. 5) and can be fitted by the equation:

$$K_{S0} = 170.9(9) - 13.0(8) \times C_{H_2O} \tag{4}$$

$$G_0 = 111.7(6) - 7.8(4) \times C_{H_2O} \tag{5}$$

where K_{S0} is the adiabatic bulk modulus in GPa, G_0 is the shear modulus and C_{H_2O} is the H_2O weight percentage. As discussed previously, nominally anhydrous wadsleyite of previous studies may contain 50 ppm or more water by weight (Jacobsen et al., 2005). The extrapolated bulk modulus for anhydrous wadsleyite is in a good agreement with previous data (Sawamoto et al., 1984; Zha et al., 1997; Liu et al., 2005) (Fig. 5). The extrapolated shear modulus for anhydrous wadsleyite is consistent with or slightly lower than previous values (Sawamoto et al., 1984; Zha et al., 1997; Liu et al., 2005).

According to (4) and (5), 1 wt.% H_2O corresponds to a 7.6% decrease in K_{S0} and a 7.0% decrease in G_0. Using available data for other olivine polymorphs and assuming a linear relationship between aggregate elastic moduli and water content, the effect of H_2O on olivine and ringwoodite can also be estimated. For hydrous olivine, 1 wt.% H_2O would correspond to a 2.9% decrease in K_{S0} and a 1.6% decrease in G_0 (Jacobsen et al., 2006). For hydrous ringwoodite, 1 wt.% H_2O corresponds to a 4.7% (Wang et al., 2003) to 7.4%

Table 2
Aggregate (VRH average) elastic moduli and wave velocities of hydrous wadsleyite

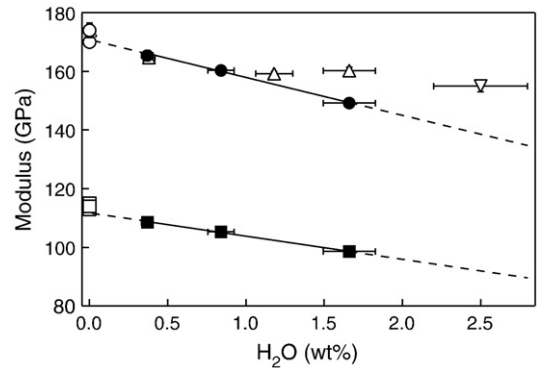|	H_2O (wt.%)	K_{S0} (GPa)	G_0 (GPa)	V_P (km/s)	V_S (km/s)
an-hw [a]	0	174(3)	114(1)	9.69(5)	5.73(3)
an-hw [b]	0	170(2)	115(2)	9.65(5)	5.75(5)
WH833	0.37(4)	165.4(9)	108.6(6)	9.48(2)	5.61(2)
WH2120	0.84(8)	160.3(7)	105.3(6)	9.36(2)	5.54(2)
SS0401	1.66(17)	149.2(6)	98.6(4)	9.09(2)	5.39(1)

[a] Sawamoto et al. (1984).
[b] Zha et al. (1997).

Fig. 5. Adiabatic bulk and shear moduli as a function of H_2O content. Solid circles and squares: this study; open circles and squares: for anhydrous wadsleyite (Sawamoto et al., 1984; Zha et al., 1997; Li et al., 2001); open upper triangles: isothermal bulk modulus of wadsleyite from Holl et al. (in press); open down triangles: Yusa and Inoue (1997). Solid line is a least-squares fit to the present data (dashed where extrapolated). Error bars are smaller than symbols when not shown.

(Inoue et al., 1998) decrease in K_{S0} and a 5% decrease in G_0 (Inoue et al., 1998; Wang et al., 2003). Thus, at least for Fe-free compositions, incorporation of water appears to have greater effect on the bulk and shear moduli of wadsleyite than for olivine and ringwoodite. For density, 1 wt.% H_2O in wadsleyite leads to a 1.3% decrease in density.

The olivine to wadsleyite phase transition is generally accepted as the main source of the 410-km seismic discontinuity in the mantle. Seismic studies typically show about a 5–6% increase in density and a 4–6% increase in seismic velocity across this boundary (Dziewonski and Anderson, 1981; Grand and Helmberger, 1984; Mechie et al., 1993; Kennett et al., 1995). At ambient conditions, the velocity contrast between anhydrous olivine and wadsleyite is 12–13% (Sawamoto et al., 1984). If such a velocity contrast persisted to 410-km depth, the corresponding olivine fraction needed to produce a velocity jump that will match seismic data would be about ~40% (Sawamoto et al., 1984; Duffy et al., 1995). Petrological models of the mantle often favor an olivine-rich composition (~60% by vol.) for the upper mantle. For such a composition to satisfy seismic data, the velocity contrast between olivine and wadsleyite should be only about 6.7–8.3%. In detail, mineralogical modeling of the 410-km discontinuity requires taking into account relative changes in velocity with P and T, Fe distribution between olivine and wadsleyite, presence of other phases, etc (Duffy and Anderson, 1989; Duffy et al., 1995; Liu et al., 2005). Even with such effects, hydration of wadsleyite has frequently been invoked to reconcile the seismic
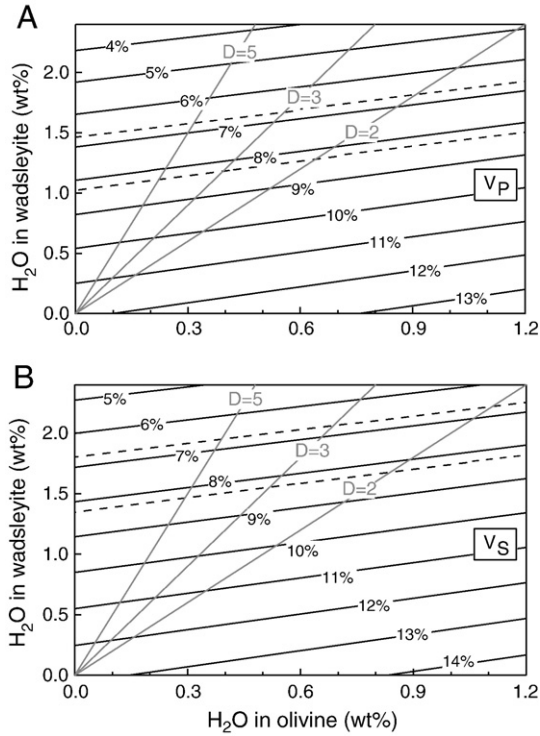
Fig. 6. Contours of velocity contrast between wadsleyite and forsterite as a function of water content at ambient conditions. Dashed lines show a velocity contrast of 6.3–8.7% which is the range required for an olivine-rich (60 vol.%) mantle to satisfy seismic data. Gray lines show corresponding H_2O contents of wadsleyite and olivine for different H_2O partition coefficients, $D_{H_2O}^{wd-ol} = 5$.

properties at 410-km depth and mineral physics data for olivine polymorphs with an olivine-rich mantle (Sawamoto et al., 1984; Chambers et al., 2005).

Using our new elasticity data together with that of Jacobsen et al. (2006), we can now directly quantify the effect of H_2O on the velocity contrast between olivine and wadsleyite. Seismic velocities were calculated for the simple case of an Fe-free system at ambient conditions and the velocity contrast between olivine and wadsleyite is plotted as a function of water content in wadsleyite and olivine in Fig. 6. Results for compressional and shear waves are similar. The presence of 1.1–1.4 wt.% H_2O in wadsleyite can reduce the velocity contrast to 7–8% if olivine is anhydrous. Alternatively, if the H_2O content of olivine is 0.8 wt.%, then an H_2O content in wadsleyite of 1.3–1.8 is needed to reduce the velocity contrast to 7–8%. Recent studies have estimated that the wadsleyite/forsterite H_2O partition coefficient is in the range of 2–5 under mantle conditions (Chen et al., 2002; Hirschmann et al., 2005; Frost and Dolejš, 2007). Values of the velocity contrast between wadsleyite and olivine are indicated for this

range of partitioning values in Fig. 6. If $D_{H_2O}^{wd-ol} = 5$, then 1.1–1.4 wt.% H_2O in wadsleyite is needed to reduce the olivine/wadsleyite velocity contrast to below 8.3%. For $D_{H_2O}^{wd-ol} = 5$, the corresponding amount of H_2O in wadsleyite is 1.2–1.5 wt.%. These water contents are close to or exceed the estimated storage capacity of the mantle at these depths (Demouchy et al., 2005), although the actual mantle water content may be less. These results indicate that the presence of H_2O can affect not only the thickness of the 410-km discontinuity (Chen et al., 2002; Hirschmann et al., 2005; Frost and Dolejš, 2007) but also the magnitude of the velocity change between the two phases. However, water contents must approach expected saturation values in order for the effects of water to reduce the velocity contrast at 410 km to the values required to match an olivine-rich (pyrolite) mantle.

4.2. Comparison with static compression data

The isothermal bulk modulus, K_T, was calculated from our measured adiabatic bulk modulus, K_S, using:

$$K_T = K_S/(1 + \alpha\gamma T) \qquad (6)$$

where T is temperature, α is thermal expansion coefficient (Inoue et al., 2004) and γ is the Gruneisen parameter (assumed to be identical to anhydrous wadsleyite (Chopelas, 1991)). The resulting K_{T0} is listed in Table S3 in the Appendix and compared with previous static compression results.

The calculated K_{T0} for 2.5 wt.% H_2O content extrapolated from this study is 13.3% lower than the value given by Yusa and Inoue (1997). For the 0.37 wt.% H_2O sample, the K_{T0} estimated in this study is close to the value given by Holl et al. (in press) (fixed $K'_{T0} = 4.0$). But for the 1.66 wt.% H_2O sample, the K_{T0} estimated in this study is 4.3% ($K'_{T0} = 5.4(11)$) or 8.5% (fixed $K'_{T0} = 4.0$) lower than the value given by Holl et al. (in press). In static compression studies, there is a trade-off between the fitted isothermal bulk modulus K_{T0} and its pressure derivative K'_{T0}. It is notable that other static compression studies on hydrous olivine polymorphs (Smyth et al., 2004, 2005; Manghnani et al., 2005) suggest high H_2O contents lead to an increase of K'_{T0}.

Using the third-order Birch–Murnaghan equation, we fitted equations of state for hydrous β-Mg_2SiO_4 with water content 0.37 wt.%, 1.66 wt.% and 2.5 wt.% (Fig. 7). V_0 was directly determined by static compression studies (Yusa and Inoue, 1997; Holl et al., in press). K_{T0} was calculated according to (4) and (6) in this study.
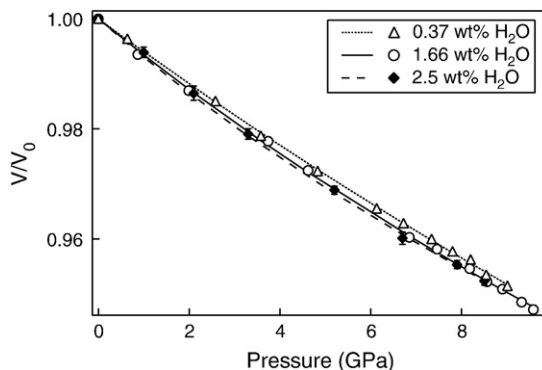
Fig. 7. Equation of state of hydrous wadsleyite. Solid, dashed and dotted lines show fits with V_0, K_{T0} constrained from X-ray and Brillouin data. Fitting results for K'_{T0} are given in Table S3 in the Appendix. Static compression data for sample containing 2.5 wt.% H_2O are from Yusa and Inoue (1997); data for 0.37 wt.% and 1.66 wt.% H_2O are from Holl et al. (in press). Error bars are smaller than symbols when not shown.

V_0 and K_{T0} were fixed during the fitting. The results for K'_{T0} are given in Table S3 in the Appendix, and the resulting compression curve is shown in Fig. 7. For the 0.37 wt.% H_2O sample, K'_{T0} is close to 4 and consistent with static compression results (Holl et al., in press). For high-water contents, incorporation of constraints from Brillouin data suggests K'_{T0} may be larger than 4. Direct measurements of elastic constants at high pressures are needed to test this hypothesis.

4.3. Bulk and shear moduli of minerals in the olivine system

Fig. 8 summarizes existing data on the bulk and shear moduli of olivine polymorphs as a function of density at ambient conditions. The figure focuses mainly on single-crystal data. The density increase for a given polymorph (solid lines in Fig. 8) reflects incorporations of iron along the solid solution. The shear modulus for all the three phases shows a monotonic decrease with density. The bulk modulus for both olivine and ringwoodite increases weakly with density following similar trends. However, the bulk modulus of wadsleyite decreases with density over the limited compositional range available. Also, the shear modulus of wadsleyite decreases more strongly with Fe than those of the other two polymorphs. Recent results from polycrystalline ultrasonic for elastic moduli of ringwoodite as a function of Fe content are also shown in the figure (short-dashed line) (Higo et al., 2006). The compositional trends differ from single-crystal data and the reasons for these differences need further investigation.

The figure also shows the variation of K_{S0} and G_0 across the three polymorphs for fixed composition (dashed lines). This is a demonstration of the validity of Birch's law (Birch, 1961) for this system. The open symbols in Fig. 8 show the adiabatic bulk and shear moduli of hydrous olivine polymorphs as well as the minerals chondrodite and clinohumite. Incorporating water produces a change in density and mean atomic weight without a major structure change. It is clear from Fig. 8 that hydrous olivine polymorphs tend to follow the structural trend (dashed lines) indicated in the
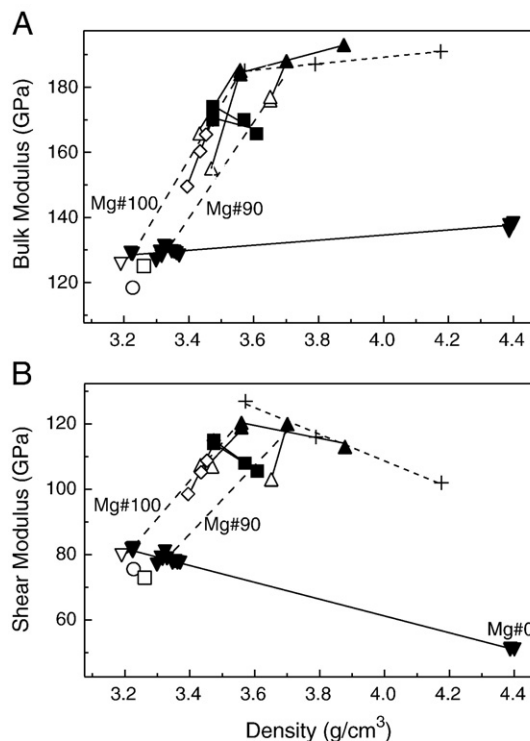

Fig. 8. Birch plots showing variation of bulk and shear moduli as a function of density for olivine polymorphs from single-crystal elasticity data at ambient conditions. Solid down triangle: anhydrous olivine (Verma, 1960; Graham and Barsch, 1969; Kumazawa and Anderson, 1969; Ohno, 1976; Sumino et al., 1977; Sumino, 1979; Suzuki et al., 1983; Graham et al., 1988; Brown et al., 1989; Isaak et al., 1989; Webb, 1989; Isaak, 1992; Yoneda and Morioka, 1992; Zaug et al., 1993; Abramson et al., 1997; Speziale et al., 2004); open down triangle: hydrous olivine (Jacobsen et al., 2006); solid square: anhydrous wadsleyite (Sawamoto et al., 1984; Zha et al., 1997; Sinogeikin et al., 1998; Katsura et al., 2001); diamond: hydrous wadsleyite (this study); solid upper triangle: anhydrous ringwoodite (Weidner et al., 1984; Sinogeikin et al., 1997; Jackson et al., 2000; Sinogeikin et al., 2003); open upper triangle: hydrous ringwoodite (Inoue et al., 1998; Wang et al., 2003; Jacobsen et al., 2004; Jacobsen and Smyth, 2006); circle: chondrodite (Sinogeikin and Bass, 1999;); open square: clinohumite (Fritzel and Bass, 1997); short-dashed line and cross: polycrystalline ultrasonic data for anhydrous ringwoodite (Higo et al., 2006).

figure. That is, the effect of water incorporation is generally consistent with the predictions of Birch's Law for both the bulk and shear modulus.

5. Conclusions

The single-crystal elasticity of hydrous wadsleyites containing 0.37 wt.%, 0.84 wt.%, and 1.66 wt.% H_2O were measured by Brillouin scattering at ambient conditions. All individual C_{ij}s decrease approximately linearly as a function of water content. The bulk and shear moduli also decrease linearly with water content according to the relation (in GPa): $K_{S0} = 170.9(9) - 13.0(8)C_{H_2O}$, $G_0 = 111.7(6) - 7.8(4)C_{H_2O}$, where C_{H_2O} is the H_2O weight percentage. For Mg_2SiO_4 olivine polymorphs, incorporation 1 wt.% H_2O in wadsleyite corresponds to a 7.6% reduction in K_{S0} and 7.0% reduction in G_0. The effect of water on the elasticity of wadsleyite is greater than for olivine and ringwoodite. Compressional, V_P, and shear velocities, V_S, of hydrous wadsleyite range from 9.48 to 9.09 km/s and 5.61 to 5.39 km/s, respectively for H_2O content between 0.37 and 1.66 wt.%.

The contrast in compressional and shear wave velocity between wadsleyite and olivine was calculated as a function of H_2O content at ambient conditions. Using an estimated H_2O partition coefficient of 3, the velocity contrast between the two phases decreases from 12 to 13% under anhydrous conditions to 7–8% when wadsleyite contains 1.3–1.6 wt.% H_2O for compressional velocity, 1.6–1.9 wt.% H_2O for shear velocity.

Acknowledgements

Appendix A. Supplementary data

Supplementary data associated with this article can be found, in the online version, at doi:10.1016/j.epsl.2007.10.045.

References

Abramson, E.H., Brown, J.M., Slutsky, L.J., Zaug, J., 1997. The elastic constants of San Carlos olivine to 17 GPa. J. Geophys. Res. 102, 12253–12263.

Birch, F., 1961. Compositions of the earth's mantle. Geophys. J. R. Astr. Soc. 4, 295–311.

Brown, J.M., Slutsky, L.J., Nelson, K.A., Cheng, L.T., 1989. Single-crystal elastic constants for San Carlos peridot: an implication of impulsive stimulated scattering. J. Geophys. Res. 94, 9485–9492.

Chambers, K., Deuss, A., Woodhouse, J.H., 2005. Reflectivity of the 410-km discontinuity from PP and SS precursors. J. Geophys. Res. 110, B02301.

Chen, J.H., Inoue, T., Weidner, D.J., Wu, Y.J., Vaughan, M.T., 1998. Strength and water weakening of mantle minerals, olivine, wadsleyite and ringwoodite. Geophys. Res. Lett. 25, 575–578.

Chen, J.H., Inoue, T., Yurimoto, H., Weidner, D.J., 2002. Effect of water on olivine–wadsleyite phase boundary in the $(Mg, Fe)_2SiO_4$ system. Geophys. Res. Lett. 29, 1875.

Chopelas, A., 1991. Thermal properties of β-Mg_2SiO_4 at mantle pressures derived from vibrational spectroscopy: implications for the mantle at 410 km depth. J. Geophys. Res. 96, 11,817–11,829.

Demouchy, S., Deloule, E., Frost, D.J., Keppler, H., 2005. Pressure and temperature-dependence of water solubility in Fe-free wadsleyite. Am. Mineral. 90, 1084–1091.

Duffy, T.S., Anderson, D.L., 1989. Seismic velocities in mantle minerals and the mineralogy of the upper mantle. J. Geophys. Res. 94, 1895–1912.

Duffy, T.S., Zha, C.S., Downs, R.T., Mao, H.K., Hemley, R.J., 1995. Elasticity of forsterite to 16 GPa and the composition of the upper mantle. Nature 378, 170–173.

Dziewonski, A.M., Anderson, D.L., 1981. Preliminary reference earth model. Phys. Earth Planet. Inter. 25, 297–356.

Every, A.G., 1980. General closed-form expressions for acoustic waves in elastically anisotropic solids. Phys. Rev., B 22, 1746–1760.

Fritzel, T.L.B., Bass, J.D., 1997. Sound velocities of clinohumite, and implications for water in earth's upper mantle. Geophys. Res. Lett. 24, 1023–1026.

Frost, D.J., Dolejš, D., 2007. Experimental determination of the effect of H_2O on the 410-km seismic discontinuity. Earth Planet. Sci. Lett. 256, 182–195.

Graham, E.K., Barsch, G.R., 1969. Elastic constants of single-crystal forsterite as a function of temperature and pressure. J. Geophys. Res. 74, 5949–5960.

Graham, E.K., Schwab, J.A., Sopkin, S.M., Takei, H., 1988. The pressure and temperature dependence of the elastic properties of single-crystal fayalite Fe_2SiO_4. Phys. Chem. Miner. 16, 186–198.

Grand, S.P., Helmberger, D.V., 1984. Upper mantle shear structure of North America. Geophys. J. R. Astron. Soc. 76, 399–438.

Higo, H.J., Inoue, T., Li, B.S., Irifune, T., Liebermann, R.C., 2006. The effect of iron on the elastic properties of ringwoodite at high pressure. Phys. Earth Planet. Inter. 159, 276–285.

Hirschmann, M.M., 2006. Water, melting, and the deep earth H_2O cycle. Annu. Rev. Earth Planet. Sci. 34, 629–653.

Hirschmann, M.M., Aubaud, C., Withers, A.C., 2005. Storage capacity of H_2O in nominally anhydrous minerals in the upper mantle. Earth Planet. Sci. Lett. 236, 167–181.

Holl, C.M., Smyth, J.R., Jacobsen, S.D., Frost, D.J., Effects of hydration on the structure and compressibility of wadsleyite, β-(Mg_2SiO_4), Am. Mineral. in press.

Hu, J.Z., Mao, H.K., Shu, J., Hemley, R.J., 1993. High pressure energy dispersive x-ray diffraction technique with synchrotron radiation.

In: Schmidt, S.C., Shaner, J.W., Samara, G.A., Ross, M. (Eds.), High-Pressure Science and Technology. New York, pp. 441–444.

Huang, X.G., Xu, Y.S., 2005. S. I. Karato, Water content in the transition zone from electrical conductivity of wadsleyite and ringwoodite. Nature 434, 746–749.

Inoue, T., Weidner, D.J., Northrup, P.A., Parise, J.B., 1998. Elastic properties of hydrous ringwoodite (-phase) in Mg₂SiO₄. Earth Planet. Sci. Lett. 160, 107–113.

Inoue, T., Tanimoto, Y., Irifune, T., Suzuki, T., Fukui, H., Ohtaka, O., 2004. Thermal expansion of wadsleyite, ringwoodite, hydrous wadsleyite and hydrous ringwoodite. Phys. Earth Planet. Inter. 143–144, 279–290.

Isaak, D.G., 1992. High-temperature elasticity of iron-bearing olivines. J. Geophys. Res. 97, 1871–1885.

Isaak, D.G., Anderson, O.L., Goto, T., Suzuki, I., 1989. Elasticity of single-crystal forsterite measured to 1700-K. J. Geophys. Res. 94, 5895–5906.

Jackson, J.M., Sinogeikin, S.V., Bass, J.D., 2000. Sound velocities and elastic properties of –Mg₂SiO₄ to 873 K by Brillouin spectroscopy. Am. Mineral. 85, 296–303.

Jacobsen, S.D., 2006. Effect of water on the equation of state of nominally anhydrous minerals. In: Keppler, H., Smyth, J.R. (Eds.), Water in nominally anhydrous minerals. Reviews in Mineralogy and Geochemistry, vol. 62. Mineralogical Society of America, Chantilly, Virginia, pp. 321–342.

Jacobsen, S.D., Smyth, J.R., 2006. Effect of water on the sound velocities of ringwoodite in the transition zone. In: Jacobsen, S.D., van der Lee, S. (Eds.), Earth's Deep Water Cycle. American Geophysical Union, pp. 131–145.

Jacobsen, S.D., Smyth, J.R., Spetzler, H., Holl, C.M., Frost, D.J., 2004. Sound velocities and elastic constants of iron-bearing hydrous ringwoodite. Phys. Earth Planet. Inter. 143–144, 47–56.

Jacobsen, S.D., Demouchy, S., Frost, J.D., Ballaran, T.B., Kung, J., 2005. A systematic study of OH in hydrous wadsleyite from polarized FTIR spectroscopy and single-crystal X-ray diffraction: oxygen sites for hydrous storage in earth's interior. Am. Mineral. 90, 61–70.

Jacobsen, S.D., Jiang, F., Smyth, J., Duffy, T.S., Mao, Z., Holl, C.M., Frost, D.J., 2006. Sound velocities of hydrous olivine and the effects of water on the equation of state of nominally anhydrous minerals. In: EOS Trans. AGU (Ed.), Fall Meet. Suppl., Abstract, 87(52). V53F-03.

Karato, S.I., 2006. Influence of hydrogen-related defects on the electrical conductivity and plastic deformation of mantle minerals: a critical review. In: Jacobsen, S.D., van der Lee, S. (Eds.), Earth's Deep Water Cycle. American Geophysical Union, pp. 113–130.

Katsura, T., Mayama, N., Shouno, K., Sakai, M., Yoneda, A., Suzuki, I., 2001. Temperature derivatives of elastic moduli of (Mg0.91Fe0.09)₂SiO₄ modified spinel. Phys. Earth Planet. Inter. 124, 163–166.

Kennett, B.L.N., Engdahl, E.R., Buland, R., 1995. Constraints on seismic velocities in the earth from travel-times. Geophys. J. Int. 122, 108–124.

Kleppe, A.K., Jephcoat, A.P., Olijnyk, H., Slesinger, A.E., Kohn, S.C., Wood, B.J., 2001. Raman spectroscopic study of hydrous wadsleyite (β-Mg₂SiO₄) to 50 GPa. Phys. Chem. Miner. 28, 232–241.

Kohlstedt, D.L., Keppler, H., Rubie, D.C., 1996. Solubility of water in the α, β and γ phases of (Mg, Fe)₂SiO₄. Contrib. Mineral. Petrol. 123, 345–357.

Kudoh, Y., Inoue, Y., 1999. Mg-vacant structural modules and dilution of the symmetry of hydrous wadsleyite, β-Mg₂₋ₓSiH₂ₓ with 0.00 ≤ × ≤ 0.25. Phys. Chem. Miner. 26, 382–388.

Kumazawa, M., Anderson, O.L., 1969. Elastic moduli, pressure derivatives and temperature derivatives of single-crystal olivine and single-crystal forsterite. J. Geophys. Res. 74, 5961–5972.

Li, B.S., Liebermann, R.C., Weidner, D.J., 2001. P–V–VP–VS–T measurements on wadsleyite to 7 GPa and 873 K: implications for the 410-km seismic discontinuity. J. Geophys. Res. 106, 30579–30591.

Libowitzky, E., Rossman, G.R., 1997. An IR absorption calibration for water in minerals. Am. Mineral. 82, 1111–1115.

Liu, W., Kung, J., Li, B., 2005. Elasticity of San Carlos olivine to 8 GPa and 1073 K. Geophys. Res. Lett. 32, L16301.

Manghnani, M.H., Amulele, G., Smyth, J.R., Holl, C.M., Chen, G., Prakapenka, V., Frost, D.J., 2005. Equation of state of hydrous Fo₉₀ ringwoodite to 45 GPa by synchrotron powder diffraction. Mineral. Mag. 69, 317–323.

Mechie, J., Egorkin, A.V., Fuchs, K., Ryberg, T., Solodilov, L., Wenzel, F., 1993. P-wave mantle velocity structure beneath northern Eurasia from long-range recordings along the profile quartz. Phys. Earth Planet. Inter. 79, 269–286.

Nye, J.F., 1985. Physical Properties of Crystals. Cambridge, Oxford.

Ohno, I., 1976. Free vibration of a rectangular parallelepiped crystal and its application to determination of elastic constants of orthorhombic crystals. J. Phys. Earth 24, 355–379.

Ohtani, E., Mizobata, H., Yurimoto, H., 2000. Stability of dense hydrous magnesium silicate phases in the systems Mg₂SiO₄–H₂O and MgSiO₃–H₂O at pressures up to 27 GPa. Phys. Chem. Miner. 27, 533–544.

Press, W.H., Flannery, B.P., Teukolsky, S.A., Vetterling, W.T., 1988. Numerical Recipes in C: The Art of Scientific Computing. Cambridge University Press.

Sawamoto, H., Weidner, D.J., Sasaki, S., Kumazawa, M., 1984. Single-crystal elastic properties of the modified spinel (beta) phases of magnesium orthosilicate. Science 224, 749–751.

Shimizu, H., 1995. High-pressure Brillouin scattering of molecular single-crystals grown in a diamond-anvil cell. In: Senoo, M., Suito, K., Kobayashi, T., Kubota, H. (Eds.), High Pressure Research on Solids. Elsevier Science, Netherlands, pp. 1–17.

Sinogeikin, S.V., Bass, J.D., 1999. Single-crystal elastic properties of chondrodite: implications for water in the upper mantle. Phys. Chem. Miner. 26, 297–303.

Sinogeikin, S.V., Bass, J.D., Kavner, A., Jeanloz, R., 1997. Elasticity of natural majorite and ringwoodite from the catherwood meteorite. Geophys. Res. Lett. 24, 3265–3268.

Sinogeikin, S.V., Katsura, T., Bass, J.D., 1998. Sound velocities and elastic properties of Fe-bearing wadsleyite and ringwoodite. J. Geophys. Res. 103, 20,819–20,825.

Sinogeikin, S.V., Bass, J.D., Katsura, T., 2003. Single-crystal elasticity of ringwoodite to high pressures and high temperatures: implications for 520 km seismic discontinuity. Phys. Earth Planet. Inter. 136, 41–66.

Smyth, J.R., 1987. β-Mg₂SiO₄: a potential host for water in the mantle? Am. Mineral. 72, 1051–1055.

Smyth, J.R., 1994. A crystallographic model for hydrous wadsleyite (β-β-Mg₂SiO₄): an ocean in the earth's interior? Am. Mineral. 79, 1021–1024.

Smyth, J.R., Frost, D.J., 2002. The effect of water on the 410-km discontinuity: an experimental study. Geophys. Res. Lett. 29, 1485.

Smyth, J.R., Kawamoto, T., Jacobsen, S.D., Swope, R.J., Hervig, R.L., Holloway, J.R., 1997. Cyrstal structure of monoclinic hydrous wadsleyite [β-(Mg,Fe)₂SiO₄]. Am. Mineral. 82, 270–275.

Smyth, J.R., Holl, C.M., Frost, D.J., Jacobsen, S.D., 2004. High pressure crystal chemistry of hydrous ringwoodite and water in the earth's interior. Phys. Earth Planet. Inter. 143, 271–278.

Smyth, J.R., Holl, C.M., Langenhorst, F., Laustsen, H.M.S., Rossman, G.R., Kleppe, A., McCammon, C.A., Kawamoto, T., van Aken, P.A., 2005. Crystal chemistry of wadsleyite II and water in the earth's interior. Phys. Chem. Miner. 31, 691–705.

Speziale, S., Duffy, T.S., 2002. Single-crystal elastic constants of fluorite (CaF_2) to 9.3 GPa. Phys. Chem. Miner. 29, 465–475.

Speziale, S., Duffy, T.S., Angel, R.J., 2004. Single-crystal elasticity of fayalite to 12 GPa. J. Geophys. Res. 109, B12202.

Sumino, Y., 1979. The elastic constants of Mn_2SiO_4, Fe_2SiO_4, Co_2SiO_4 and the elastic properties of olivine group minerals at high temperature. J. Phys. Earth 27, 209–238.

Sumino, Y., Nishizawa, O., Goto, T., Ohno, I., Ozima, M., 1977. Temperature variation of elastic constant of single-crystal forsterite between −190 and 400 °C. J. Phys. Earth 25, 377–392.

Suzuki, I., Anderson, O.L., Sumino, Y., 1983. Elastic properties of a single-crystal forsterite Mg_2SiO_4 up to 1,200 K. Phys. Chem. Miner. 10, 38–46.

Verma, R.K., 1960. Elasticity of some high-density crystals. J. Geophys. Res. 65, 757–766.

Wang, J.Y., Sinogeikin, S.V., Inoue, T., Bass, J.D., 2003. Elastic properties of hydrous ringwoodite. Am. Mineral. 88, 1608–1611.

Webb, S., 1989. The elasticity of the upper mantle orthosilicates olivine and garnet to 3 GPa. Phys. Chem. Miner. 16, 684–692.

Weidner, D.J., Sawamoto, H., Sasaki, S., Kumazawa, M., 1984. Single-crystal elastic properties of the spinel phase of Mg_2SiO_4. J. Geophys. Res. 89, 7852–7860.

Wood, B.J., 1995. The effect of H_2O on the 410-kilometer seismic discontinuity. Science 268, 74–76.

Yoneda, A., Morioka, M., 1992. Pressure derivatives of elastic constants of single-crystal forsterite. In: Syono, Y., Manghnani, M.H. (Eds.), High Pressure Research: Applications to Earth and Planetary Sciences, vol. 3. American Geophysical Union, Washington D.C., pp. 207–214.

Yusa, H., Inoue, T., 1997. Compressibility of hydrous wadsleyite (β-phase) in Mg_2SiO_4 by high pressure X-ray diffraction. Geophys. Res. Lett. 24, 1831–1834.

Zaug, J.M., Abramson, E.H., Brown, J.M., Slutsky, L.J., 1993. Sound velocities in olivine at earth mantle pressures. Science 260, 1487–1489.

Zha, C.S., Duffy, T.S., Downs, R.T., Mao, H.K., Hemley, R.J., 1996. Sound velocity and elasticity of single-crystal forsterite to 16 GPa. J. Geophys. Res. 101, 17,535–17,545.

Zha, C.S., Duffy, T.S., Mao, H.W., Downs, R.T., Hemley, R.J., Weidner, D.J., 1997. Single-crystal elasticity of β-Mg_2SiO_4 to the pressure of the 410 km seismic discontinuity in the earth's mantle. Earth Planet. Sci. Lett. 147, E9–E15.